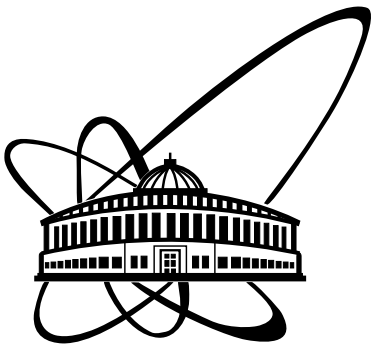

Nucleation Theory and Applications

Jürn W. P. Schmelzer, Gerd Röpke, and Vyatcheslav B. Priezzhev (Editors)

Dubna JINR 2006

5 Dynamical Clustering in Chains of Atoms with Exponential Repulsion

Alexander P. Chetverikov[(1,2)], *Werner Ebeling*[(1,3)] *and Manuel G. Velarde*[(1)]

[(1)] *Instituto Pluridisciplinar, Universidad Complutense, Paseo Juan XXIII, 1, 28040 Madrid, Spain*

[(2)] *Physical Faculty, Chernychevsky State University, 410012 Saratov, Russia*

[(3)] *Institut für Physik, Humboldt Universität, Newtonstr. 15, 12489 Berlin, Germany*

Personally I'm always ready to learn, although I do not always like being taught.

Sir Winston Churchill

Abstract

We investigate the dynamical clustering in chains of atoms with Morse-type interactions at higher densities, where the exponential repulsion dominates and the structure is lattice-like. First we study several mechanisms to generate and stabilize soliton-like dynamical clusters. Although, generally, clusters are unstable, yet, there exist dynamical clusters with finite lifetime, which are due to local compressions running along the chain. We show that these dynamical, metastable clusters may give rise to significant physical effects. In order to study the effects of dynamical clusters on electrical transport we assume that each atom may generate a free electron which is able to move on the lattice. Their motion is described in a classical approximation. The dynamical clusters (localized compressions)

running along the chain may interact with the electron system and influence their motion creating some extra electronic current.

5.1 Introduction

For the case of one dimension (1D) several problems of statistical physics were solved exactly [1, 2]. In several recent papers we developed the statistical thermodynamics of chains with Morse-type interactions [3, 4, 5]. In particular we investigated the clustering problem in low density Morse systems. A cluster was defined as a local density peak, which is relatively stable with respect to collisions. Here we concentrate on higher densities where the exponential repulsion dominates and the configuration is lattice-like. The usual equilibrium clusters are unstable due to the strong interactions. However as we will show, there exist dynamic clusters, representing running local compressions, which are soliton-like. We will investigate here the generation and the properties of these dynamic clusters moving along the lattice. Further we discuss the influence of dynamic clustering on electrical transport. In recent communications [6, 7] the present authors have already discussed, albeit in a sketchy way, the possibility of soliton-mediated electric conductance phenomena in a lattice with Toda interactions. Here we will study also the influence of dynamic clustering on electron dynamics.

5.2 Models of Interaction with Exponential Repulsion

The Morse potential was introduced in 1929 by P. Morse in a paper with the title "Diatomic molecules according to wave mechanics" [8]. In this fundamental work Morse treated the problem of atomic interactions at small distances and derived a simple expression for the quantum interactions between atoms. The potential depends on two parameters B, D and reads in its general form

$$U^M(r) = D\left[(\exp(-B(r-\sigma))-1)^2 - 1\right] . \tag{5.1}$$

The potential has a minimum at $r = \sigma$ and may be considered as a good alternative to the well-known model of Lennard-Jones

$$U^{L-J}(r) = \frac{B}{r^{12}} - \frac{A}{r^6} . \tag{5.2}$$

The long range part of the Morse potential is less realistic than the $1/r^6$ term in the Lennard-Jones potential, however the exponential repulsion term in the Morse potential is well founded on quantum-mechanical calculations. The predominant cause of exponential repulsion between atoms is the wave functions overlapping of the valence electrons and is created mostly in the region close to the axis between the atoms [9].

The repulsive part of the Morse potential is identical to the exponential potential studied by Toda [10]

$$U^T(r) = \frac{a}{b}\exp(-b(r-\sigma)) \; . \tag{5.3}$$

This potential, as well as a modification with an additional (unphysical) linear term, was treated in great detail by Toda [10]. The characteristic frequency connected with the Toda potential is

$$\omega_0^2 = \frac{ab}{m} \; , \tag{5.4}$$

where m is the mass of the particles [10].

A useful combination between the Toda- and the Lennard-Jones potentials is the Buckingham (exp6) potential

$$U^B(r) = \frac{D}{10}\left[6\exp(-b(r-\sigma)) - 16\left(\frac{\sigma}{r}\right)^6\right] \tag{5.5}$$

that describes well realistic cases [11]. Since simulations with an r^{-6}-tail may give rise to numerical difficulties (due to the long range which often is avoided by setting a cut-off at some finite distance) we work here with the Morse potential which has an exponentially decaying attracting tail. In order to be consistent with the notation for the exponential potential, we introduce here a (generalized) Morse potential in the following form

$$U^M(r) = \frac{a}{b}\left[\exp(-b(r-\sigma)) - 2\alpha\exp\left(-\frac{b}{2}(r-\sigma)\right)\right] \; . \tag{5.6}$$

In the region of higher densities the first term dominates and the second one, which is proportinal to a parameter α, will give only a small correction. The potential has a minimum at

$$r = r_{min} = \sigma - \frac{2}{b}\ln\alpha \; . \tag{5.7}$$

The potential crosses zero at the distance

$$r_c = \sigma - \frac{2}{b}\ln(2\alpha)\ . \tag{5.8}$$

For $r < r_c$, the repulsive part grows exponentially with the stiffness b. In the simplest case $\alpha = 1$ we recover the standard Morse potential in the form of Eq. (5.1) with $B = 2b$ and $D = a/b$. In this case we get $r_{min} = \sigma$ and the characteristic frequency of oscillations around the minimum is given by

$$\omega_1^2 = \frac{ab}{2m}\ . \tag{5.9}$$

The exponential repulsive part of the interaction forces models the Pauli repulsion between the overlapping valence shells of the atoms. The Morse potential may be considered as a quite realistic model for atomic interactions for both repulsive as well as attractive interactions.

The evolution of anharmonic lattices with Morse interactions, in short Morse chains, has been studied [3, 4, 5] including particle clustering, thermodynamical and kinetic transitions. Most of the mentioned work was devoted to chains with relative low density, where the attractive part of the Morse interactions dominates the dynamics. Here we will focus attention on the opposite case of relatively high density. We shall discuss the excitations and their possible influence on electrical transport. In particular we will study the coupling between dynamical clusters and electrical charges in ionized chains.

5.3 Nonlinear Dynamics of Morse Chains

First we will study the dynamics of a 1D Morse-type atomic lattice consisting of N atoms with periodic boundary conditions. We will disregard any ionization phenomena. Let us assume that the mean distance between the Morse particles is $r_0 = L/N$ where L and N are, respectively, the length and the number of particles in the chain. We will study now the forces acting on a particle. Take a Morse particle placed midway between two other nearest neighbor Morse particles separated by the average distance $2r_0$. If the displacement from the center is denoted by x the effective potential felt by the central particle is (see Fig. 5.1)

$$U_{eff}^M = \frac{2a}{b}\left[\exp(b(\sigma - r_0))\cosh(bx) - 2\alpha\exp\left(\frac{b}{2}(\sigma - r_0)\right)\cosh\left(\frac{b}{2}x\right)\right]\ . \tag{5.10}$$

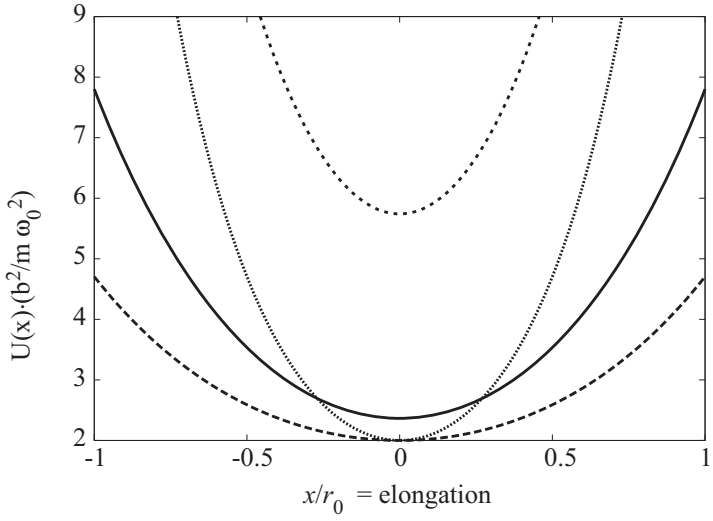

Fig. 5.1 Morse lattice: Effective potential acting on a given particle placed between two other Morse particles at distance $2r_0$. We compare with the case of a pure exponential potential $\alpha = 0$, corresponding to the density $r_0 = \sigma$; the two curves for the exponential case corresponding to the stiffness $b\sigma = 3$ or $b\sigma = 4$ respectively touch the abscissa. The two other curves correspond to a Morse chain with $\alpha = 1$ and to a two times higher density of particles $r_0 = \sigma/2$, the stiffness is $b\sigma = 3$ or $b\sigma = 4$ respectively.

In the following we shall omit the superscript M. We see that an exponential potential with the density $r_0 = \sigma$ leads to quite similar effective interactions as the proper Morse potential with the double density $r_0 = \sigma/2$. Clearly the inner particle is bound to experience quasilinear oscillations around the minimum for small excitations or large elongations depending on the nonlinear terms.

In the presence of random forces and also external forces the dynamics of particles with mass m in the chain is described by the Langevin equations ($k = 1, 2, \ldots, N$)

$$\frac{d}{dt}x_k = v_k \ , \qquad \frac{d}{dt}v_k + \gamma_0 v_k + \frac{\partial U}{m\partial x_k} = \frac{1}{m}F_k(r_k, v_k)) + \sqrt{2D}\,\xi_k(t) \ , \tag{5.11}$$

governing the stochastic motion of the k-th particle on the ring. The stochastic forces $\sqrt{2D}\,\xi_k(t)$ model a surrounding heat bath (Gaussian white noise).

The potential energy stored in the ring reads

$$U = \sum_{k=1}^{N} U_k(r_k) \; . \tag{5.12}$$

The term γ_0 describes the standard friction frequency acting on the atoms in the chain from the side of the surrounding heat bath. The validity of an Einstein relation is assumed [3]

$$D = k_B T \gamma_0 / m \; . \tag{5.13}$$

Here T is the temperature of the heat bath. Note that there exist several other temperature concepts [5].

The force F_k acting on the chain of particles may include external driving as well as interactions with host particles (like the electrons) imbedded into the chain. First we studied the basic excitations when $F_k = 0$, $\gamma_0 = 0$, and $D = 0$. We consider a linear chain of $N = 10$ masses m located on a ring; this is equivalent to a chain with periodic boundary conditions. The particles are described by coordinates $x_j(t)$ and velocities $v_j(t)$, $j = 1, \ldots, N$, i.e.

$$x_{k+N} = x_k + L \; . \tag{5.14}$$

First we assumed that the mean density of the particles $r_0 = N/L$ is near to the equilibrium distance r_{min}. Then we may linearize the potential, hence approximating the potential Eq. (5.6) by linear springs. We introduce the deviations from it $r_j = x_{j+1} - x_j - r_{min}$ (relative mutual displacements) and find in the case of small amplitudes

$$U_i(r_j) = \frac{m}{2} \omega_1^2 r_j^2 \; , \tag{5.15}$$

corresponding to a harmonic pair interaction potential. For N masses connected by linear springs without external noise and friction we get the following linear system of dynamical equations for the displacements from equilibrium positions u_j

$$\frac{d^2}{dt^2} u_j + \omega_1^2 \left(u_{j+1} + u_{j-1} - 2u_j \right) = 0 \; . \tag{5.16}$$

The basic solution of this system reads

$$u_j^{(n)}(t) = A\cos(\omega_n t - jk_n\sigma) \ . \tag{5.17}$$

As well known there exist N different excitations corresponding to different wave lengths and the corresponding wave numbers

$$-\frac{N}{2} < n \leq +\frac{N}{2} \tag{5.18}$$

or wave "vectors" k_n

$$-\frac{\pi}{\sigma} < \frac{2\pi n}{N\sigma} \leq +\frac{\pi}{\sigma} \ . \tag{5.19}$$

This is the so-called Brillouin zone.

We remind that k-values in the region $k \pm (2\pi/\sigma)$ are equivalent due to the 2π-periodicity of the $\cos(x)$. The spectrum of eigen frequencies corresponding to linear collective vibrations which are the phonons is

$$\omega_n = \pm 2\omega_1 \sin\left(\frac{\sigma}{2}k_n\right) \ . \tag{5.20}$$

The spectrum of phonons characterized this way is also called the acoustical branch. The frequency increases with the k-value.

There exists a second more complicated case, where the elementary excitations may be treated analytically. This is the case of high density $r_0 \ll \sigma$, when the Morse chain is determined by the exponential repulsion of the particles. Then the chain is equivalent to N point masses m connected at both sides by exponentially repulsive springs corresponding to the case $\alpha = 0$. As already mentioned, the characteristic frequency is given by the Toda frequency $\omega_0 = \sqrt{ab/m}$. As we know from the Toda theory of the uniform infinite Toda lattice this system possesses solutions representing cnoidal waves and soliton-type solutions [10]. Soliton solutions represent stable local excitations. They generate local energy spots which are running along the lattice. For a uniform chain $b_n = b, (-\infty < n < \infty)$ Toda found the following exact integrals of the Hamiltonian equations [10].

$$\exp\left(-b(r_{j+1} - r_j)\right) = \text{const} \cdot Z(2K(k))Z\left(\omega_0 t \pm jk\right) \ . \tag{5.21}$$

Here $Z(u)$ and $K(k)$ represent elliptic integrals or elliptic functions respectively [10] (for simplicity we assume here units with $\sigma = 1$).

By adjusting appropriately the periodic boundary conditions for the N particles we find N normal modes, which are the nonlinear generalizations of the phonon modes found before. For the special case of an infinite lattice one of the solutions reduces to

$$\exp\left(-b(r_{j+1}-r_j)\right) = 1 + \sinh^2(\chi)\mathrm{sech}^2\left(\chi j - \frac{t}{\tau}\right) . \tag{5.22}$$

These solitonic excitations correspond to local compressions of the lattice with

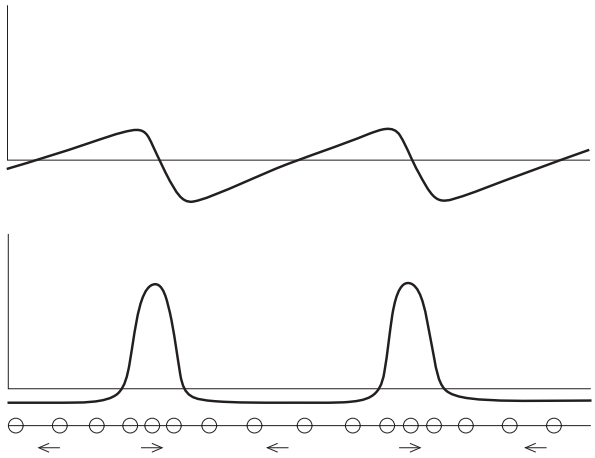

Fig. 5.2 Toda lattice: Bottom: particle motions; center: the soliton function, top: first derivative of the soliton function

the characteristic compression time

$$\tau_{sol} = (\omega \sinh\chi)^{-1} \tag{5.23}$$

and with the spatial "width" χ^{-1}. This quantity is connected with the energy of the soliton by

$$E^{sol} = 2\epsilon(\sinh\chi\cosh\chi - \chi) . \tag{5.24}$$

As the energy unit we will take the energy of an oscillator with the frequency ω_0 and the amplitude σ connected via

$$\epsilon = \omega_0^2\sigma^2 . \tag{5.25}$$

Here again σ serves as the unit of length.

Toda's solution Eq. (5.22) represents a compression wave running along the chain. In the following we will use the function

$$C_j(t) + 1 = \exp[-b(r_j - r_{j-1})] = \exp[-b(x_{j+1} - 2x_j + x_{j-1})] \tag{5.26}$$

for characterizing the local strength of the solitonic pulse at site j. For ideal Toda solitons

$$C_j(t) = \sinh^2(\chi)\mathrm{sech}^2\left(\chi(j-1) - \frac{t}{\tau}\right) \tag{5.27}$$

holds. For deformed (real) solitons we expect a shape similar to a Toda soliton pulse Eq. (5.22).

The soliton energy is determined only by the initial conditions and a soliton in a conservative lattice lives forever. In our case however, the dissipative aspects may play an important role, so we are going to study this aspect now in more detail.

5.4 Excitation of Running Local Compressions: Dynamical Clusters

5.4.1 Driving Solitons by External Forcing

The solutions presented so far solve the Hamiltonian equations in two limiting cases. Let us study now the generation of excitations in a dissipative system including friction and noise by forcing the elements. The aim is to force the masses $j = 1, \ldots, N$ in such a way that the wanted excitations are generated. The forcing introduces energy into the system which in a stationary state has to be compensated by friction. We take the previous dynamical equations of Newtonian type, introduce friction forces and external spatial and time periodic forces resulting in the following set of equations

$$\begin{aligned} &\frac{d}{dt}x_j = v\ , \qquad j = 1, \ldots, N\ , \\ &m\frac{d}{dt}v_j = F_j(t) - \frac{\partial U}{\partial x_j} - m\gamma_0 v_j\ . \end{aligned} \tag{5.28}$$

In the case of small motions around r_{min} we may linearize. In order to generate phonons (or even cnoidal waves) of order n we may apply the forcing

$$F_j^{(n)}(t) = F_0 \Omega_n^2 \cos(\Omega_n t - j k_n \sigma + \phi) \tag{5.29}$$

with $\Omega_n \simeq \omega_n$. As we will show, in general, the value of the frequency for excitation should be a little bit higher than the value predicted by the dispersion relation for the linear case $\Omega_n \geq \omega_n$.

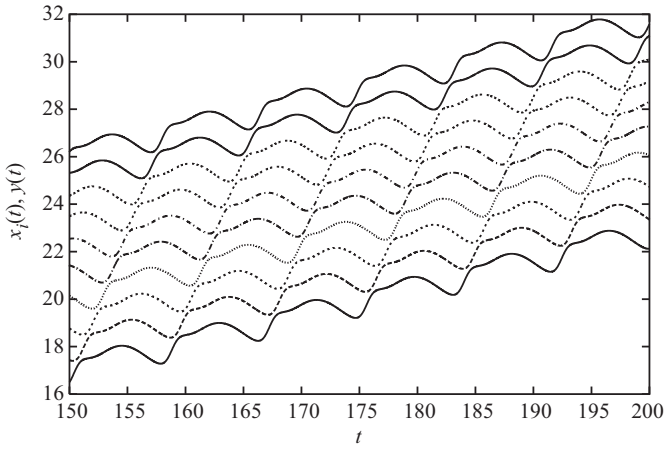

Fig. 5.3 The ten trajectories corresponding to a forced soliton in a *passive* nonlinear lattice with $b = 2$, $a = 1$, $a_1 = 0$, $\gamma_0 = 0.2\omega_0$, $F_0 = 0.15$. We show the trajectories of ten particles and demonstrate that one soliton per unit cell is excited

The physical realization of such a forcing is not trivial. We may think about a piezoelectric material in which the chain is imbedded, a kind of "waveguide". In this "waveguide" we may induce running excitations of the wanted type with given k_n and correspondingly adapted Ω_n, which by an appropriate coupling are transferred to the chain.

We first consider the case of small amplitudes and linearized equations. In this case the dispersion relation will be obeyed exactly, $\Omega_n = \omega_n$. It can be shown that the driven system possesses an attractor given by

$$x_j^{(n)}(t) = A_0 \cos(\omega_n t - j k_n \sigma + \Phi) \tag{5.30}$$

with stable amplitudes and phases. A similar procedure works also for cnoidal waves. However in this case the dispersion relation has to be found numerically.

The differential equations Eq. (5.11) have been integrated by means of a fourth-order Runge-Kutta algorithm adapted for solving stochastic problems [12]. We used $l_0 = \sigma$ as the length unit and $t_0 = 1/\omega_0 = (m/ab)^{1/2}$ as the time unit. We show in Fig. 5.3 the trajectories of a 10-particle exponential lattice (periodic boundary conditions) with a running external forcing according to Eq. (5.29). The stiffness is $b = 2$, and the amplitude of the force is $F_0 = 0.15$, correspondingly, we are in the nonlinear regime. Being in the nonlinear regime, the dispersion relation Eq. (5.20) is no longer valid. According to the dispersion relation we expect for the solitonic mode $\omega_1 = 0.57\omega_0$ and a velocity corresponding to the velocity of sound v_s. In order to generate a solitonic mode we need a k-value corresponding to this mode. The frequency of the exciting wave should be somewhat higher than the value estimated from the dispersion relation for the linear case. The appropriate value for k which should be also used in the excitation wave is

$$k_1 = \frac{2\pi}{10\sigma} \simeq 0.628 \; . \tag{5.31}$$

Then the corresponding appropriate frequency is $\omega_{ex} = 0.82\omega_0$.

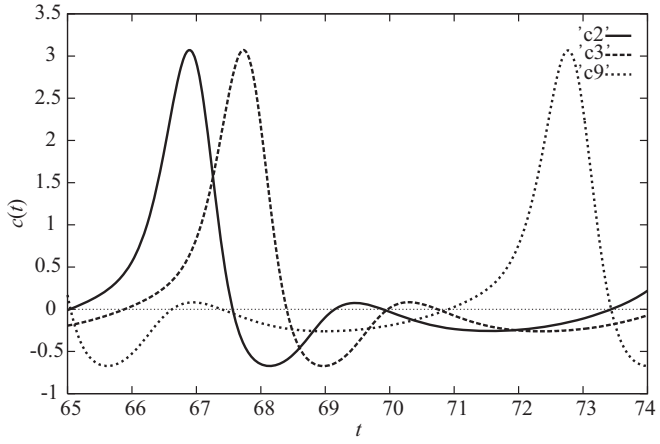

Fig. 5.4 The functions $C_i(t)$ characterizing the soliton strength for the sites $i = 2, 3, 9$. The functions correspond to the forced soliton described in Fig. 5.3

In Fig. 5.4 we depict the local shape of the soliton $C_i(t)$ as defined above for the sites $i = 2, 3, 9$. We see that the pulse is indeed running along the lattice. The height of the pulse is a measure of the soliton strength which is determined here by the strength of forcing. We see that the pulse has indeed a similar shape as Toda's function Eq. (5.27). In other words, the excitation created by the forcing remains soliton-like. In difference to Toda's function we observe that the forced excitation (Fig. 5.3) shows some "tails" (see Fig. 5.4).

5.4.2 Excitation of Solitons by Stochastic Initial Conditions and Stabilization by *Active* Friction

We consider now systems without external forcing $F_k = 0$ (Fig. 5.5) using initial conditions created by stochastic disturbance. We may think about a realization by sudden heating and quenching. We use a Gaussian distribution of the particle velocities corresponding to a high-temperature Maxwellian as initial condition of the order of $k_B T_{in} \simeq 0.1$ (in units of the energy of harmonic oscillations with amplitude σ). This is near to the critical temperature $k_B T_{cr} \simeq 0.16$, where we are in the soliton-generating region [17]. Besides other excitations many solitons are generated. However they are difficult to recognize due to the random motions of the particles. Then we quench to a temperature near to zero. The solitons survive since they have a higher lifetime than most other excitations. Looking at the trajectories we observe the expected nonlinear soliton-like excitations that decay after a time of the order $t_{rel} \simeq 1/\gamma_0$ (Fig. 5.5). These excitations exist also under equilibrium conditions [17].

In order to sustain the solitonic excitations for a longer time interval we applied as in earlier works an active Rayleigh friction in the period after heating and quenching. Then the soliton regime becomes a stable attractor [4, 18, 19] and can be studied for a longer time (driven solitons appear in the lattice). In order to provide the energetic support to soliton-like excitations we used the velocity-dependent active friction function

$$F_1(v_k) = m_i \gamma_{i0} \left(\delta - \frac{v_k^2}{v_d^2} \right) v_k \ , \tag{5.32}$$

where δ is a bifurcation parameter ($\delta = 0$ corresponds to the passive case).

The effects of active friction force were investigated in more detail in our earlier work [5]. For the passive regime $\delta = 0$ the deterministic dynamics has a single

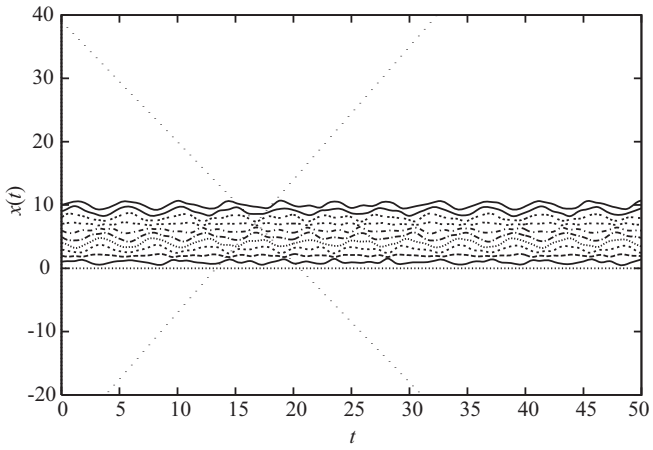

Fig. 5.5 Metastable cnoidal (solitonic) waves: As a result of quenching of an initial state with $T(0) \simeq 0.1$ the trajectories of ten particles generate soliton-like excitations, which are represented by the slopes of the wavy trajectorries

attractor at $v = 0$. Without noise all particles come to rest at $v = 0$. For $\delta > 0$ the point $v = 0$ becomes unstable but there are now two additional zeros at

$$v = \pm v_0 = v_1 \sqrt{\delta - 1} \, . \tag{5.33}$$

These two velocities are the new attractors of the free deterministic motion if $\delta > 0$.

In recent work [6, 7] it was shown that electrons may be coupled to the driven solitons and form rather stable dynamic bound states with the solitons ("solectrons"). This effect will be studied again in the next section.

5.5 Dynamics of Electrons Coupled to Running Local Compressions

5.5.1 Semiclassical Model of Electron Dynamics

In order to study the possible influence of dynamical clusters of the type described above on electric conduction we will assume now that the atoms can be ionized

emitting one free electron to a kind of "band" and leaving a negative ion. In other words, in the modified model we imbedded N electrons between the N ionic masses on the chain. To describe the dynamics of the electrons we stay on a classical level similar as the early conductance theories of Drude, Lorentz and Debye. We mention quantum-meachanical approaches to related problems by Davydov, Hennig and others [14, 15, 16].

For simplicity we start here with Langevin equations for N electrons (mass m_e, charge $-e$) and N ions (mass m_i, charge $+e$) moving on a lattice of length $L = N\sigma$ with $m_e \ll m_i$ and periodic boundary conditions. Take the N electrons located at the positions y_j moving in the nonuniform, and, in general, time-dependent electric field generated by the positive chain particles located at x_k.

The electron-electron interaction, which results from Coulomb repulsion, Heisenberg uncertainty, and Pauli's exclusion principle, is modelled here in a rather crude way. We take into account that at small distances the effective potential is linear before it approaches at larger distances the classical Coulomb interaction [7]

$$\begin{aligned} U_{ee}(r) &= U_{ee}(0) - \frac{e^2}{\lambda^2} r + O(r^2) \ , \\ U_{ee}(r) &= 0 \qquad \text{if} \qquad r > \frac{U_{ee}(0)\lambda^2}{e^2} \ , \end{aligned} \tag{5.34}$$

where

$$\lambda = \frac{\hbar}{\sqrt{m k_B T}} \tag{5.35}$$

is the de Broglie thermal wave length of the electrons. This leads to a rather weak constant repulsive force at small distances

$$F_{ee} = F_0 = \frac{e^2}{\lambda^2} = \text{const} \ , \tag{5.36}$$

which is much weaker than a purely classical Coulomb repulsion. The repulsive force F_{ee} acts between any pair of nearest neighbor electrons and keeps them away from clustering. Due to the weak influence of the electron-electron repulsion we neglected it in most calculations.

We assume that the chain particles are atomic ions or atoms with an ionic core. In order to simplify the description, we decribe the electron-ion interaction by a

Coulomb potential with an appropriate cut-off as often used e.g. in plasma theory [7, 22]

$$U_{ek}(r_{jk}) = (ee_k\kappa) - \sum_k \frac{ee_k}{\sqrt{r_{jk}^2 + h^2}} \qquad \text{if} \qquad r_{jk} < r_1 \tag{5.37}$$

and

$$U_{ek}(r_{jk}) = 0 \qquad \text{if} \qquad r_{jk} > r_1 \ , \tag{5.38}$$

where $r_{jk} = y_j - x_k$ is the distance between the electron and its neighbors in the chain and $1/\kappa$ as well as r_1 play the role of an appropriate "screening length" [7]. Here our choice is $r_1 = 3\sigma/4$ and $\kappa = 2/\sigma$. Further $-e$ is the electron charge and e_k the charge of the ion core of the chain particles. We introduced h as a free parameter which determines the short-range cut-off of the Coulombic pole, an appropriate choice is $h \simeq 0.3\sigma$.

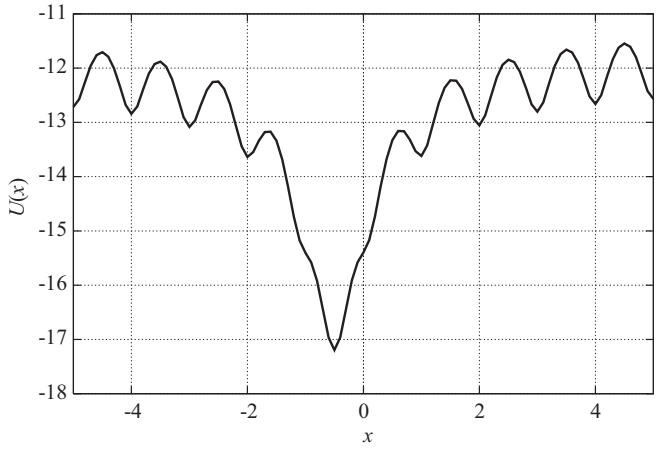

Fig. 5.6 Typical configuration of the local electric field created by the solitonic excitation. The minimum corresponds to a local compression of ions which means an enhanced charge density

Similar pseudo-potentials were introduced first by Hellman and are of current use in solid state theory [13]. The choice of the concrete value of "height" of the pole is made such that the electrons are only weakly bound to the ion cores and may

tunnel from one side of an ion to the other one. Accordingly the electrons are able to transit from one to the other side of an ion and yield an electron current. For the electron dynamics we take a classical "Drude-Lorentz-Debye dynamics"

$$\frac{dv_j}{dt} + \sum_k \frac{\partial U_e(y_j)}{m_e \partial y_j} = -\gamma_{e0} v_j + \sqrt{2D_e}\,\xi_k(t)\ . \tag{5.39}$$

The evolution of the electrons is assumed to be passive (i.e. damping for all velocities), including white noise. The stochastic forces, $\sqrt{2D_e}\,\xi_j(t)$, model a surrounding heat bath (Gaussian white noise), obeying a fluctuation-dissipation theorem. Note that the friction acting on the electron is small $m_e\gamma_e \ll m\gamma_0$. The character of the electron dynamics depends on h and on the positions of the ions. Our choice $h \simeq 0.3\sigma$ allows to generate strong local minima at the positions of strong (soliton-like) compressions (see Fig. 5.6).

Several of the assumptions made here with respect to the electrons are not very realistic. However what matters here only is the principal effect. We wanted to show, how the dynamical clusters created by solitonic excitations act on the electrons. A quantum-mechanical tratment of the electron dynamics within the tight-binding approximation is presented elsewhere [16]; it has been shown there that the essential effects described in the present work are not influenced by the approximations.

5.5.2 Coupling Between Soliton Modes and Electron Dynamics

In order to study the coupling of electrons to the lattice vibrations we will consider long trajectories of the electronic positions and velocities, $v_j^e = \dot{y}_j$. We measure the energy (temperature) in units $U_0 = m\omega_0^2\sigma^2$, fixed $b\sigma = 1$ and taking $e^2/(m\sigma) = 0.2U_0$. All computations start with the initial state of equal distances between ions.

The initial velocities of the ions were randomly taken from a Gaussian distribution with amplitude v_{in}. Initially each electron is placed midway between two ions at rest, $v_{e,l} = 0$. Differential equations Eqs. (5.39) have been integrated by means of a fourth-order Runge-Kutta algorithm adapted for solving stochastic problems [12]. We used $l_0 = \sigma$ as the length unit and $t_0 = 1/\omega_0 = (m_i/ab)^{1/2}$ as the time unit. Our assumption that the initial velocities of the ions were randomly taken from a normal distribution corresponds to an initial Maxwell distribution and therefore to an initial temperature. We mention that such conditions may be reached experimentally by a heat shock applied to the lattice. The motions of ions

and electrons occur in different time scales. Heavy ions are not affected practically by light electrons and electrons move on the background of the Coulomb potential profile created by the ions. The dynamics of the ion ring leads to soliton-like excitations. Typical solitonic excitations correspond to local compressions moving on the ring. Fig. 5.6 shows a characteristic profile of the electric field created by the ion ring at certain time moment. We see a rather deep potential well moving around the ring. The light electron may be captured in this dynamic potential well and eventually may follow the soliton dynamics. In our simulations the integration step is chosen to describe correctly the fastest component of the process, the oscillations of electrons in the potential well.

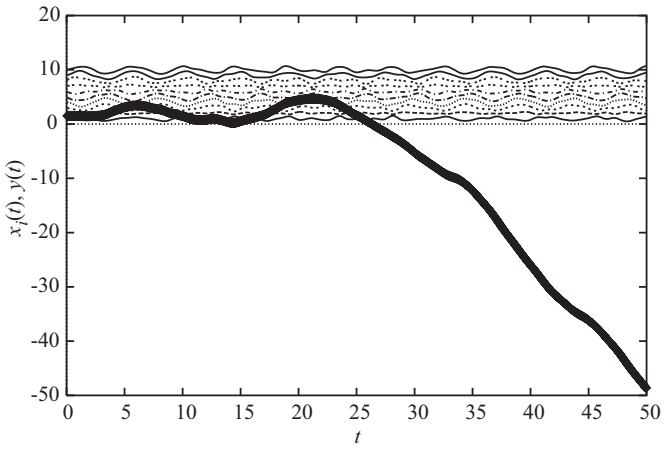

Fig. 5.7 Metastable "solectron": As a result of quenching of an initial state with $T(0) \simeq 0.1$ the trajectories of ten Toda particles (ions) generate solitons. A soliton forms a bound state with an electron captured by the soliton (a "solectron"). During this time interval the electronic trajectory is parallel to the "tangent" representing the solitonic velocity. (Parameter values: $\gamma_{i0} = \gamma_{e0} = (0.0002)/t_0$, unit of time on the abscissa, $t_0/\sqrt{5}$, unit of length on the ordinate, $l_0 = \sigma$)

In the computer experiments demonstrated in Fig. 5.7 we used an initial Gaussian distribution of the ion velocities corresponding to a high-temperature Maxwellian with $k_B T_{in} \simeq 0.1$ (in units of the energy of harmonic oscillations with amplitude σ). As in the case earlier studied, this is near to the critical temperature $k_B T_{cr} \simeq 0.16$, where we are in the soliton-generating region [17]. Besides other excitations many solitons are generated. However they are difficult to recognize

due to the random motions of the particles. Then we quenched to a temperature near to zero. The solitons survive since they have a higher lifetime than most other excitations. Looking at the trajectories we observe the expected nonlinear soliton-like excitations that decay after a time of the order $t_{rel} \simeq 1/\gamma_0$ (Fig. 5.7). These excitations exist also under equilibrium conditions [17].

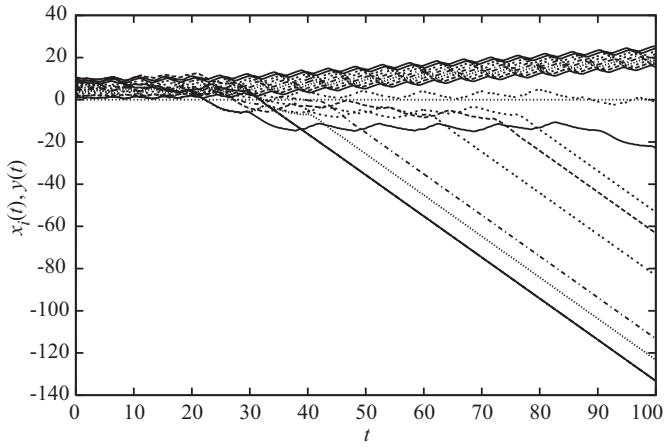

Fig. 5.8 Trajectories of 10 ions moving clockwise creating one fast dissipative soliton moving in opposite direction to the motion of the ions, and trajectories of 10 electrons captured in part by the soliton which is made stable due to the energy input ($\delta = 2$)

In order to sustain the solitonic excitations for a longer time interval we applied an active Rayleigh friction in the period after heating and quenching as described in the previous section. Then the soliton regime becomes a stable attractor [4, 18, 19]. The simulations presented below correspond to the Rayleigh approximation with $\delta = 2$, $v_d = 1$, $m/m_e = 1000$, $\gamma_0 = \gamma_{e0} = 0.2$. A soliton corresponds to a local compression of the lattice which is running opposite to the mean ion motion. This creates a charge density wave. Snapshots show that the electrons are captured by local concentrations of the ionic charge. Since the electrons search for the deepest nearby minimum of the potential, they will be most of the time located near to local ion clouds. The soliton is a dynamic phenomenon, the ions participating in the local compression are changing all the time. Hence, the electrons have always new partners for forming the "solectron".

Three stages are found: In the first one the initial state tends to one of $N + 1$

for N odd (or N in the other case) attractors [18]. The maximal average velocity among the running waves has the excitation with one local compression on the ring. The attractor, reached by the system without noise and external field, is defined mainly by the value of v_{in} given by the initial conditions. Rotations appear at very small initial velocity values. Then, upon increasing v_{in}, k-solitonic waves may be excited with increasing k. There exists always a target attractor for a given value v_{in}. For our case the initial conditions lead preferentially to the one-soliton attractor. In the absence of the external field both directions have equal probability, the field breaks the symmetry.

As mentioned above our choice for the value of a cut-off distance in the electron-ion interaction Eq. (5.36) is $h = 0.3\sigma$. In this case the difference between the maximum in the electron-ion interaction force and the corresponding value for an electron and an ion being away from the electron more than 1.5σ, is an order of magnitude lower, and hence interaction of the electron with such ions is not taken into account in the simulations. Thus we consider the interaction of each electron with the ions placed, e.g., about one third of the ring near that electron only ($N = 10$, $n_e = n_i = 1$).

To simplify, the parameters of the potentials, of the Rayleigh formula, the friction coefficients, both masses and charges of particles were held fixed. The initial velocities v_{in}, the values of the external field and the electronic temperature T_e are varied in different runs.

In Fig. 5.8 we show a simulation for the trajectories (left to right) of 10 ions creating 1 dissipative soliton which moves in opposite direction (right to left). After a transient regime, the electron is coupled to the soliton and moves approximately with the soliton velocity opposite to the motion of the ions. In the driven case ($\delta = 2$) the ions perform a constant drift. After a transient regime, solitonic excitations of the ions are formed moving with velocity v_s opposite to the average drift of the ions. Most of the electrons are captured by these dynamical clusters.

5.6 Discussion

We have shown that in dense lattices of particles with exponential repulsion, special nonlinear waves may be excited which may be interpreted as dynamical clusters - running local compressions. These dynamical clusters are similar to the cnoidal waves in Toda's theory. We have shown that these strongly localized excitations corresponding to local compressions of the chain may be generated also in dissipative lattices by external forcing, stochastic initial conditions or

negative friction. In order to measure the solitonic strength of the excitations, we introduced a special function.

We studied the properties of ionized atomic, hence electrically conducting, chains. Each atom was assumed to provide one electron moving along the chain in the field of the remaining ionic lattice. The electrons prefer positions near to the deep (electrostatic) potential wells formed by the local compression connected with the soliton. We have shown that, as time proceeds, most of the electrons are captured by such local compressions and move with the soliton velocity opposite to the ion drift. This way we have shown how significant for electric conduction is the role of localized running excitations in lattices with exponential repulsion and, in particular, the role of bound states between dynamical clusters and electrons ("solectrons").

Acknowledgment

The authors thank Dirk Hennig, Jürn Schmelzer and Boris Smirnov for useful discussions and several suggestions.

5.7 References

1. N. Bernasconi and N. D. Schneider, *Physics in One Dimension* (Winston, Philadelphia, 1976).

2. A. Scott, *Nonlinear Science* (Oxford University Press, Oxford, 1999).

3. J. Dunkel, W. Ebeling, and U. Erdmann, Eur. Phys. B **24**, 511 (2001).

4. J. Dunkel, W. Ebeling, U. Erdmann, and V. Makarov, Int. J. Bifurc. & Chaos **12**, 2359 (2002).

5. A. Chetverikov, W. Ebeling, and M. G. Velarde, Eur. Phys. J. B, **44**, 509(2005).

6. M. G. Velarde, W. Ebeling, and A. P. Chetverikov, Int. J. Bifurc. & Chaos **15**, 245 (2005).

7. A. Chetverikov, W. Ebeling, and M. G. Velarde, Contr. Plasma Phys. **45**, 275 (2005).

8. P. Morse, Phys. Rev. **34**, 57 (1929).

9. R. S. Berry and B. M. Smirnov, Phys. Rev. B **71**, 144105 (2005).

10. M. Toda, *Nonlinear Waves and Solitons* (Kluwer, Dordrecht, 1983).

11. E. M. Apfelbaum, V. S. Vorob'ev, and E. M. Martynov, Chem. Phys. Lett., in press, (2005).

12. N. N. Nikitin and V. D. Razevich, J. Comput. Math & Meth. Phys. **18**, 108 (1978).

13. N. Ashcroft and N. D. Mermin, *Solid State Physics* (Holt, Rinehardt (Eds.), Winston, Philadelphia, 1976).

14. A. S. Davydov, *Solitons in Molecular Systems* (Naukova Dumka, Kiev, 1984).

15. D. Hennig et al., Physica D **180**, 256 (2003), J. Biol. Physics **30**, 227 (2004).

16. M. G. Velarde, W. Ebeling, D. Hennig, and C. Neissner, Int. J. Bifurc. & Chaos, in press (2005).

17. W. Ebeling, A. Chetverikov, and M. Jenssen, Ukrain. J. Phys. **45**, 479 (2000).

18. V. Makarov, W. Ebeling, and M. G. Velarde, Int. J. Bifurc. & Chaos **10**, 1075 (2000).

19. V. Makarov, E. del Rio, W. Ebeling, and M. G. Velarde, Phys. Rev. E **64**, 036601 (2001).

20. E. del Rio, V. A. Makarov, M. G. Velarde, and W. Ebeling, Phys. Rev. E **67**, 056208 (2003).

21. U. Erdmann, W. Ebeling, L. Schimansky-Geier, and F. Schweitzer, Eur. Phys. J. B **15**, 105 (2000).

22. T. Pohl, U. Feudel, and W. Ebeling, Phys. Rev. E **65**, 046228 (2002).